

On the Origin of Green Emission in Polyfluorene Polymers: The Roles of Thermal Oxidation Degradation and Crosslinking**

By Wei Zhao,* Ti Cao, and John M. White*

The green emission of poly(9,9'-dioctylfluorenyl-2,7'-diyl), end-capped by polyhedral oligomeric silsequioxanes, (PFO-POSS) has been investigated by photoluminescence (PL) and photoexcitation (PE), gel permeation chromatography (GPC), and transmission Fourier transform infrared (FTIR) spectroscopy. The green emission is closely correlated with thermal oxidation degradation and crosslinking of the polymer and is enhanced by annealing at elevated temperatures. The green-to-blue emission intensity ratio, used to assess the emission properties of thin (90 nm) films, was 3.70, 4.35, and 1.54 for an air-annealed film, its insoluble residue (crosslinked), and a film cast from its soluble portion, respectively. For thick (5–6 μm) film, the ratios are 13.33, 13.33, and 0.79, respectively. However, FTIR spectroscopy of thick films leads to the conclusion that the carbonyl-to-aromatic ring concentration ratio are 0.018, 0.015, and 0.032, respectively. Focusing on the recast films, the green emission is relatively low while the carbonyl concentration is relatively high. This suggests that the energy traps at crosslinked chains play an important role in green emission. It is likely that the crosslinking enhances the excitation energy migration and energy transfer to the defects by hindering chain segment twisting.

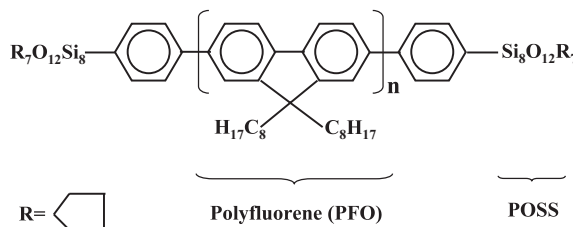
1. Introduction

Light-emitting conjugated polymers continue to attract great attention because of their potential display applications.^[1] Stable and efficient electroluminescence of three primary colors, e.g., red, green, and blue, is essential to achieve a full-color display. Although these three colors have been demonstrated in polymer light-emitting devices (PLEDs), only the red and green PLEDs seem to have reached sufficiently high efficiencies and lifetimes for commercial applications.^[2–4] Currently a major issue is degradation of blue PLEDs, leading to undesirable green emission and, thus, unsatisfactory lifetimes.^[5,6]

Poly(*para*-phenylene) (PPP)-type materials have emerged as a promising class of conjugated polymers for blue-light-emitting devices, but most PPP-based PLEDs suffer rapid degradation when used in ambient atmospheres,^[7,8] resulting in an emission wavelength change from blue (~430 nm) to green (~530 nm).^[5,6,9] Although a number of mechanisms have been suggested, the origin of the green emission remains unclear.^[9–11]

While this undesired green emission has been attributed to reordering of the polymer chains and subsequent aggregation^[10] and/or excimer formation,^[7,12–14] this interpretation is questionable since important literature reports that poly(9,9-dioctylfluorene)s (PFOs) show spectral stability when annealed in N₂ and vacuum.^[5,6] The green emission has also been linked to the oxidation of defects incorporated into the polymer backbone during PFO synthesis.^[5,6,15] There is also a valuable temperature-dependent study that rules out excimers as the source of the green emission and casts doubt on a role for aggregates.^[6] However, others have reported that binary blends of PFO and polymers with high glass-transition temperatures, *T_g*, demonstrated spectral stability.^[16] They also found that PFO segregates to the top layer of blends. Taken together, it is clear that questions remain regarding operative mechanism(s).

In the experiments described in this paper, we focus on comparing air-annealed PFO-POSS films with two films derived from them. The derived films are made from the portions of the air-annealed films that are soluble and insoluble in toluene. Films were analyzed using photoluminescence (PL) and photoexcitation (PE), gel permeation chromatography (GPC), and transmission Fourier transform infrared (FTIR) spectroscopy on poly(9,9'-dioctylfluorenyl-2,7'-diyl) end-capped, to enhance stability,^[17] by polyhedral oligomeric silsequioxanes (PFO-POSS) (Scheme 1). From these results we conclude that



Scheme 1. Molecular structure of PFO-POSS.

[*] Dr. W. Zhao,^[+] Prof. J. M. White,^[+] Dr. T. Cao
Department of Chemistry and Biochemistry
University of Texas at Austin
Austin, TX 78712 (USA)
E-mail: w_zhao@mail.utexas.edu, jmwwhite@mail.utexas.edu

[+] Second address: Center for Materials Chemistry, University of Texas at Austin, Austin, TX 78712, USA.

[**] This work was supported by the National Science Foundation (CHE0070122), the Robert A. Welch Foundation and the Center for Materials Chemistry of the University of Texas. We gratefully acknowledge Prof. S. E. Webber for allowing us to use SPEX Fluorolog-τ2 spectrofluorometer and GPC facilities in his laboratory. The FTIR data were gathered using the facilities of the Center of Nano- and Molecular (CNM) Science and Technology of the University of Texas. We gratefully acknowledge useful discussions with Barry Young, VP and CFO of DisplaySearch Corp.

thermal oxidation degradation and accompanying crosslinking of PFO plays an important role in intensifying the green emission.

2. Results and Discussion

2.1. 90 nm PFO Films

To undergird our experiments dealing with recast films, we have repeated experiments (Fig. 1) on previously reported PL and PE spectra for a) a pristine film, b) a film annealed in N₂ at 200 °C for two hours, and c) a film annealed in air at 200 °C for two hours.^[5–17] The annealing temperature is above the glass-transition temperature.^[18] In one distinction from other work, we monitored PE spectra at two wavelengths (470 and 570 nm). The spectra were each normalized at their maximum values.

As in the above-referenced reports, the PL spectra display vibronic structures in the blue-emission regime (below 510 nm); the PL spectra of the pristine film and the film annealed in N₂ are similar and dominated by blue emission (Figs. 1a,b), while green emission dominates the air-annealed

film (Fig. 1c). To compare, we take the intensity ratio, (I_{Green}/I_{Blue}), of the green emission (~530 nm) to the strongest peak of the blue emission. These ratios for the N₂-annealed and pristine films are equal (0.05) and significantly lower than for the air-annealed film (3.70).

To pursue further the role of film organizational changes, we exposed an air-annealed film to saturated toluene vapor for three hours at room temperature, then removed the solvent from the swollen film by evaporation at 60 °C in a vacuum oven. The swelling and densification associated with adding and removing toluene should alter the film organization to some degree. However, we found no change in the green-to-blue emission intensity ratio. Apparently, simply reorganizing the film is an inadequate explanation.

Turning to the PE spectra (Fig. 1), we measured the PE spectra at 470 nm (blue) and 570 nm (green) while scanning the excitation wavelength. The PE intensities increase and decrease with the PL intensities and, importantly, a scaled version of 570 nm emission profile tracks faithfully that of 470 nm emission (not shown). The latter strongly suggests that the green and blue emissions involve the same excitation process, i.e., electronic excitation of fluorene chromophores. Unlike the PL spectra, the PE spectral profiles are not altered by the annealing procedure. Apparently, even though green emission dominates for the air-annealed film, the structural changes, compared to the other two films, are minimal. This points to an alternative source—energy traps located at defects. Efficient energy migration between fluorene chromophores and energy transfer between excited fluorene chromophores to these traps lead to green emission.

In agreement with the literature, Figure 1 indicates that ambient oxygen plays a key role in green emission. To probe for oxygen-containing species in the films, we used X-ray photoelectron spectroscopy (XPS) and FTIR spectroscopy. Comparing high-resolution XPS scans of the O(1s) region indicated no surface concentration difference between pristine and air-annealed films (not shown). In the C(1s) region there were, as expected, two shake-up features.^[19] The absence of a detectable change in O(1s) shows that in the near-surface region of these films, the oxygen concentration differs by no more than 1%. Transmission FTIR spectroscopy was used to probe the bulk (and surface) of these films, giving special attention to the carbonyl stretching vibration that would indicate a role for oxidation.^[5,6] Even though the C=O stretching vibration has an extremely high cross-section in FTIR,^[20] we found no evidence for carbonyl groups in a thin (90 nm) air-annealed film. We estimate that detection of the carbonyl stretch would require a film thickness of 1 μm if 1% of the repeat units contain a carbonyl group. Thus, the absence of a detectable carbonyl concentration implies only that fewer than 10% of the repeat units contain carbonyl groups. For a 50 to 60 fold thicker air-annealed film, an upper limit of 1.8% is calculated (see below) on the basis of a weak carbonyl IR signal.

Motivated by the above results, we undertook experiments to probe in a different way for the effects of air oxidation on the chemical and physical properties of these films. We used an approach that, to our knowledge, has not been taken hereto-

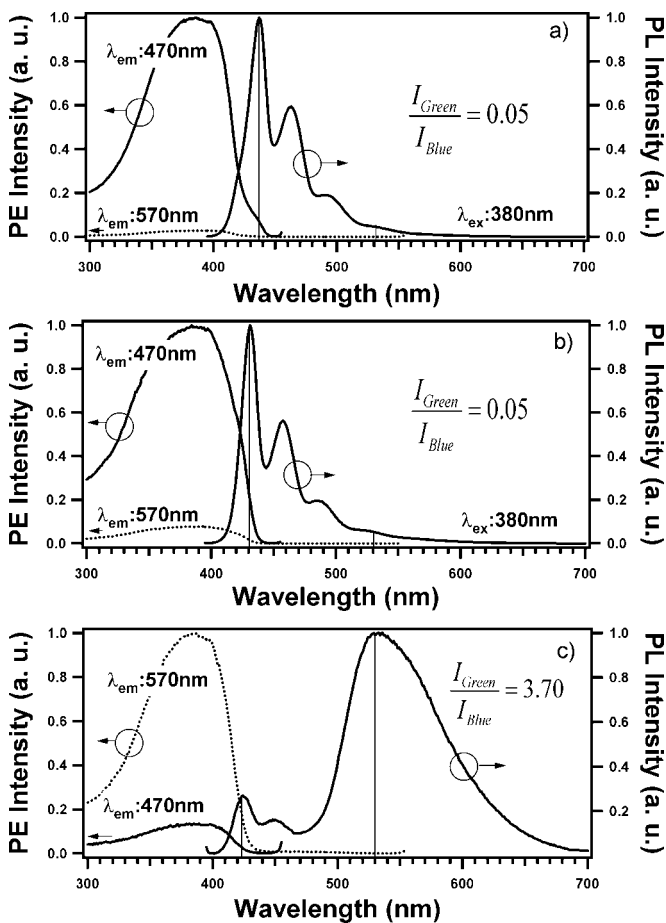


Figure 1. PL and PE spectra of 90 nm PFO-POSS films: a) pristine, b) N₂-annealed at 200 °C, and c) air-annealed at 200 °C.

fore. In this approach, we examined the solubility of pristine and air-annealed films and the PL and PE of the soluble and insoluble portions.

In one set of experiments we placed each film in 2 mL of toluene. After 24 h, the substrates were removed and dried at 60 °C in a vacuum oven. The solubilities were very different; based on XPS and FTIR spectroscopy (not shown), 97 % of the pristine film, but only 20 % of the air-annealed film, dissolved. The PL and PE spectra of the soluble and insoluble portions revealed interesting differences. For the insoluble portions, the green-to-blue PL intensity ratios (Fig. 2) are 0.22 and 4.35 for the pristine and air-annealed films, respectively. These ratios were lower (0.05 and 3.70) in both films before washing in toluene. We speculate that the origin of the factor-of-four increase for the pristine film is the result of a combination of drying at 60 °C in vacuum and standing in ambient air for roughly 1 or 2 days. The insolubility (80 %) of the air-annealed film indicates a structural change consistent, as described below, with crosslinking during annealing at 200 °C. The PL spectra indicate that the species responsible for the intense green emission are retained in this insoluble portion. Supporting the hypothesis of crosslinking to form supermacromolecular materials, we found that the portions not soluble in toluene do not dissolve in other common solvents, e.g., benzene, tetrahydrofuran (THF), chloroform, acetone, *n*-dichlorobenzene, and carbon tetrachloride.

Turning to soluble portions of these films, we measured PL spectra (Fig. 3) of solutions made by diluting the soluble portions 30-fold (to reduce self-absorption and avoid detector saturation). Comparing the soluble portions of the pristine and air-annealed films, the blue emission regions very nearly overlap but the green emission tail for the annealed film is stronger by a factor of two. This comparison indicates that the soluble portion contains a small concentration of species produced by the 200 °C air annealing.

In a follow-up experiment, we changed the solvent to benzene in order to freeze-dry soluble portions of pristine and air-annealed films. The solutions were prepared by separately dipping the films in 2 mL benzene for 24 h, removing the substrates, and freeze-drying the solutions under vacuum, forming PFO powder. Each powder was dissolved in 50 μL of toluene and the solution was dropped onto a substrate, without spinning, dried in air at room temperature then in a vacuum oven at 60 °C. Although no photo-oxidation was expected, the possibility was minimized by avoiding exposure to light during the freeze-dry process. For these recast films derived from the pristine and air-annealed samples (Fig. 4), the green-to-blue emission intensity ratios are 0.05 and 1.54, respectively. For the pristine film and the film recast from its soluble portion, the in-

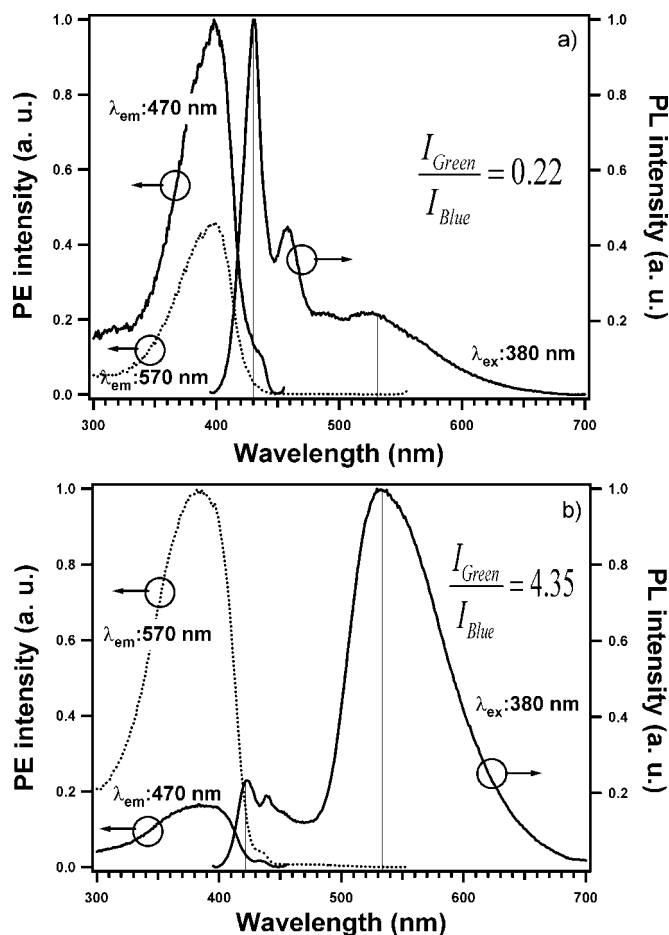


Figure 2. PL and PE spectra of the residual films after washing with toluene: a) pristine and b) air-annealed at 200 °C.

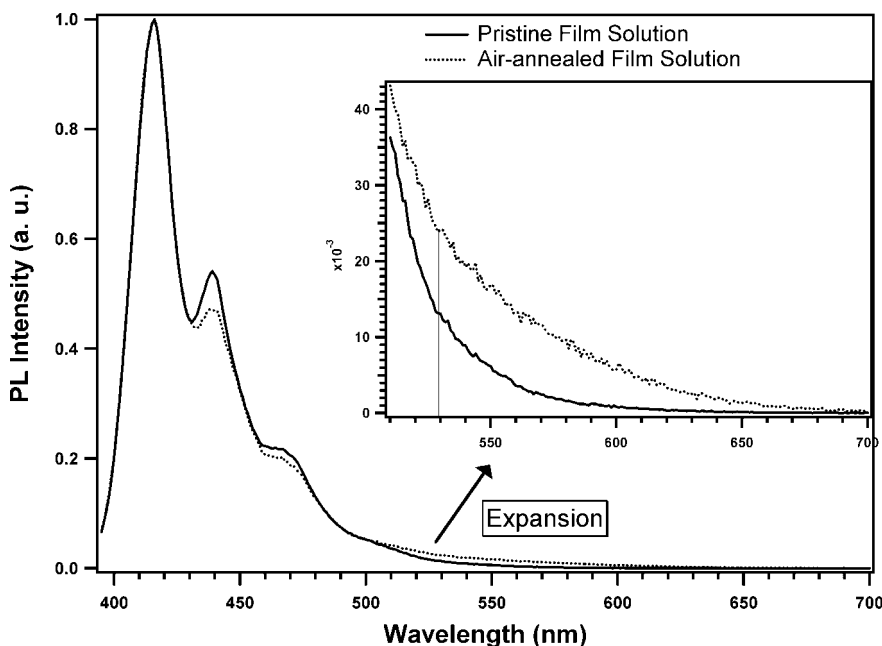


Figure 3. Solution PL spectra of diluted soluble portions of the pristine and air-annealed films.

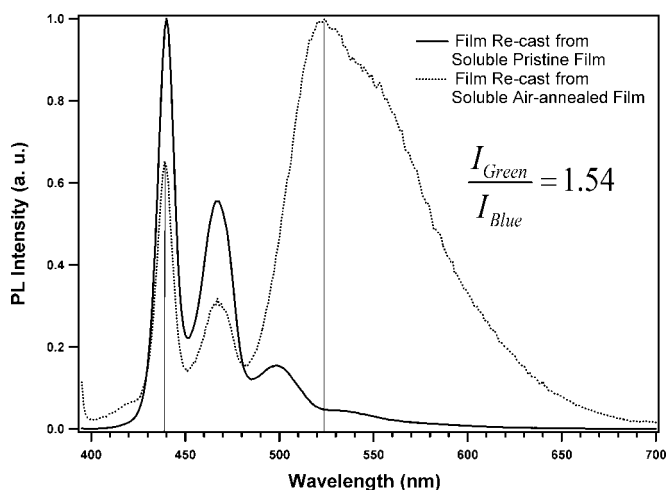


Figure 4. PL spectra of films cast from the soluble portions of the pristine and air-annealed films.

tensity ratio is the same. The analogous comparison for the air-annealed sample indicates a 58 % decrease (3.70 to 1.54) of the green emission in the film recast from its soluble portion.

Emission with 480 nm excitation is attributed to electronic excitation of fluorenone groups. Emission with 380 nm excitation is attributed to electronic excitation of the polymer backbone.^[6,12] Green emissions (490 to 700 nm) resulting from excitation at 480 and 380 nm are compared in Figure 5. Comparing the insoluble, Figure 5a, and soluble, Figure 5b, portions of the film, the green emission intensity ratio (Eq. 1) is a factor of 2.5 higher for the former.

$$I_{\text{Green}}(\lambda_{\text{ex}} \sim 380 \text{ nm}) / I_{\text{Green}}(\lambda_{\text{ex}} \sim 480 \text{ nm}) \quad (1)$$

Assuming the relative concentration of fluorenone groups is monitored by $I_{\text{Green}}(\lambda_{\text{ex}} \sim 480 \text{ nm})$ intensity, there is a factor of 2.5 stronger green emission per unit for the insoluble residue than for the soluble portion. This result indicates that factors in addition to fluorenone concentration play an important role in determining the green emission associated with excitation at 380 nm.

For the solution derived from the air-annealed sample (Fig. 3) the green-to-blue intensity ratio is less than 0.023. This is a factor of 70 less than that for the solid film (Fig. 4) made from this solution. The difference is attributed to the enhanced inter-chain energy migration and energy transfer to a small number of defects in the solid; although these defects are present in the solution, inter-chain energy migration and energy transfer are strongly suppressed. In terms of Förster energy transfer, the efficiency is proportional to $(R_0/R)^6$, where R is the distance between donor and acceptor chromophores and R_0 is determined by the overlap of the emission spectrum of the excited donors and the absorption spectrum of acceptors. Typical values of R_0 range from 1 to 4 nm and R is a comparable distance in the solid but is much longer in the diluted solu-

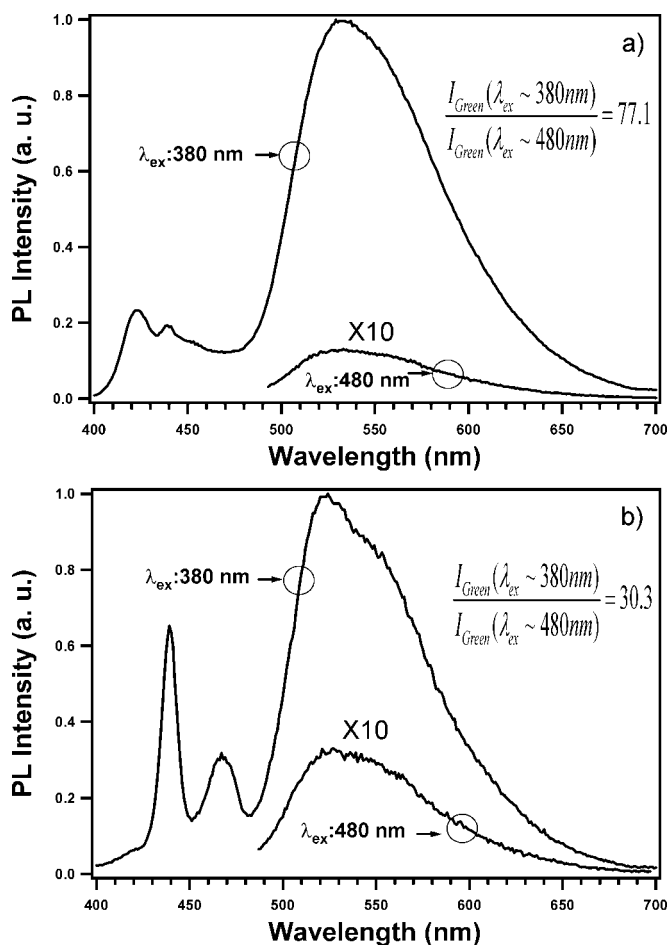


Figure 5. PL spectra of films recast from the a) insoluble and b) soluble portions at 380 and 480 nm excitations.

tion. From this perspective, a small defect concentration that has little, if any, influence on solution spectra can have a large effect in a solid film. Thus, ongoing efforts to purify PFO polymers are important.^[21]

The idea that thermal treatment, especially in air, promotes degradation and crosslinking to form both smaller and larger species, was confirmed using GPC. Solutions (50 μL) from the soluble portions of the pristine and air-annealed films were examined (Fig. 6, Table 1). Although 80 % of the air-annealed film is insoluble, the soluble portion has a larger molecular weight polydispersity ($PD = 3.15$), a higher weight-average molecular weight ($\overline{M}_w = 69\,900$), but a lower number-average molecular weight ($\overline{M}_n = 22\,200$, 53 monomer units) than the soluble portion of the pristine film ($PD = 2.23$, $\overline{M}_w = 60\,000$, and $\overline{M}_n = 27\,000$, 65 monomer units), which indicate that chain scission and consequent recombination of scission chains must occur during annealing in air. Most (80 %) of the air-annealed film is insoluble. While this precludes determination of the degree of polymerization, we conclude that it is significantly higher than for the soluble portion and is the result of crosslinking (discussed further below).

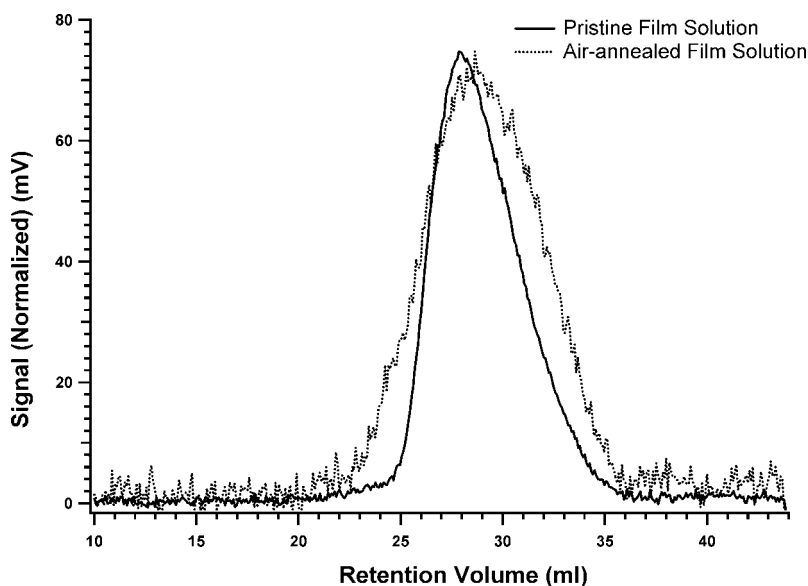


Figure 6. Gel permeation chromatography (GPC) profiles of the soluble portions of 90 nm pristine and air-annealed films (see also Table 1).

Table 1. GPC data analysis.

Experimental conditions	\bar{M}_n	\bar{M}_w	PD
Pristine film solution	26 973	60 014	2.225
200°C ambient annealed film solution	22 190	69 915	3.151

2.2. Thick PFO Films

Probing thin films by FTIR spectroscopy for carbonyl groups was limited by inadequate combination of sensitivity and sample thickness. This motivated gathering FTIR spectra of 5–6 μm thick PFO films processed in the same way as the thin films (Fig. 7). In agreement with published spectra,^[5,12,15] the C–H stretching vibrations of the alkyl chain appear at 2855 and 2926 cm^{-1} , the C–H stretching of the aromatic ring at 2953 cm^{-1} , and the aromatic ring breathing vibration at 1460 cm^{-1} . The broad peak at 1123 cm^{-1} is ascribed to the Si–O stretching vibration of the Si-containing end cap. The alkyl C–H rocking mode is at 813 cm^{-1} . In the pristine film, there are three modes not discussed in prior literature that we ascribe to alkyl chain C–H bending (1402 and 1377 cm^{-1}) and alkyl chain C–H twisting (1253 cm^{-1}). After the film was annealed in air, these three bands weakened and, importantly, an additional peak appeared at 1716 cm^{-1} , assigned to the stretching vibration of a carbonyl species that we take to be part of the polymer, e.g., some of the fluorene is oxidized to fluorenone. The weakened C–H bending and twisting is compatible with crosslinking that restricts motion in the alkyl chains.

To estimate the relative amount of fluorenone, FTIR data from Pannozzo et al.^[12] for a fluorene–fluorenone copolymer was used to calculate the molar extinction coefficient ratio of carbonyl-to-aromatic ring, ($\epsilon_{\text{C=O}}/\epsilon_{\text{Aromatic Ring}}$) = 12.5. Assuming this ratio is independent of film thickness, the carbonyl-to-aromatic ring concentration ratio calculated for the thick air-annealed film is very small (0.018).

The distribution of carbonyl-bearing species in the insoluble (Fig. 8) and soluble (Fig. 9) parts of air-annealed and pristine thick films were examined using FTIR spectroscopy. As for thin films, the pristine sample intensity is barely detectable, reflecting high solubility in toluene. The poor solubility of the air-annealed thick film is indicated by the very intense FTIR bands (Fig. 8). The calculated carbonyl-to-aromatic ring concentration ratio is 0.015 compared to 0.018 for the original film. In passing, we note that the thick pristine film delaminated upon dipping in toluene and at least part of the delaminated layer was insoluble in toluene. This supports our suggestion that PFO

slowly degrades and crosslinks at room temperature in air.

As for thin films, the portions of pristine and air-annealed thick films soluble in benzene were also recast using the freeze–dry approach. Because the solubility of the thick air-annealed films is very low (~5%), the soluble portions of several air-annealed thick films were combined to obtain sufficient material for adequate signal-to-noise in FTIR. After freeze–drying, 50 μL toluene was added to each sample to make a concentrated solution that was dropped onto a substrate, dried in air and in the vacuum oven at 60 °C overnight. Transmission FTIR spectroscopy (Fig. 9) shows no carbonyl in the film cast from the soluble part of the pristine film. In the film cast from the

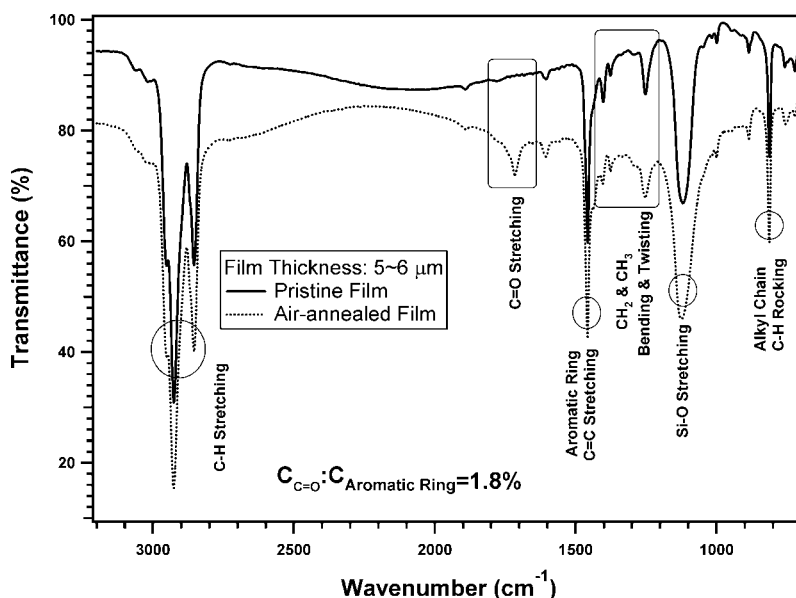


Figure 7. FTIR spectra of thick PFO-POSS pristine and air-annealed films.

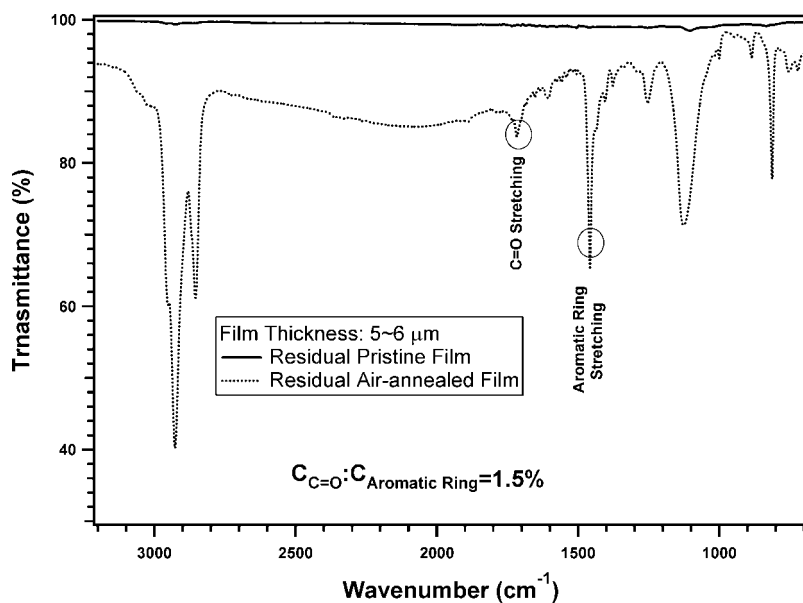


Figure 8. FTIR spectra of the insoluble portions of thick pristine and air-annealed films.

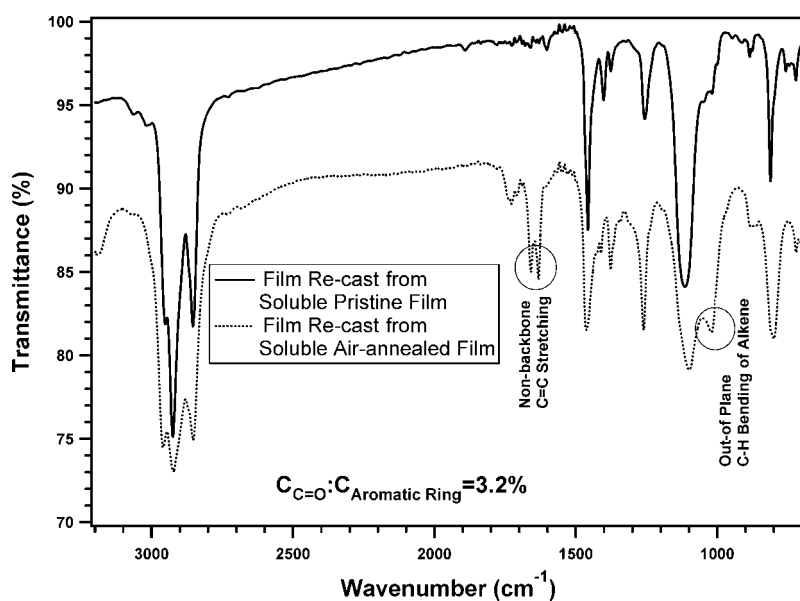


Figure 9. FTIR spectra of the films cast from the soluble parts of thick pristine and air-annealed films.

Table 2. Summary of PL and FTIR results.

Solid samples	$I_{\text{Green}}/I_{\text{Blue}}$ [a]	$I_{\text{Green}}/I_{\text{Blue}}$ [b]	$C_{\text{C=O}}/C_{\text{Aromatic Ring}}$ [c]
Pristine film	0.05	0.05	0.0
Film annealed in N_2 at $200^\circ\text{C}/2$ h	0.05	–	0.0
Film annealed in air at $200^\circ\text{C}/2$ h	3.70	13.33	0.018
Insoluble residue at $200^\circ\text{C}/2$ h annealed film	4.35	13.33	0.015
Film recast from soluble part of $200^\circ\text{C}/2$ h air-annealed film	1.54	0.79	0.032

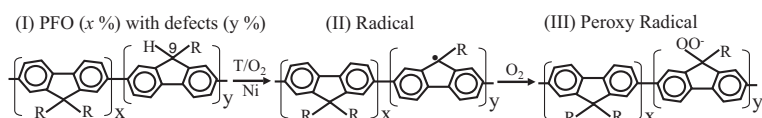
[a] Estimated from emission spectra of thin films (~ 90 nm). [b] Estimated from emission spectra of thick films ($5\text{--}6$ μm). [c] Estimated from FTIR spectra of thick films ($5\text{--}6$ μm).

soluble part of the air-annealed film, the carbonyl-to-aromatic ring concentration ratio is higher (0.032) than in the original air-annealed film (0.018) and its insoluble portion (0.015). Compared to the original film and its insoluble portion, there are new peaks for the film cast from the soluble part—a pair (1430 and 1460 cm^{-1}) attributed to C=C double-bond stretching not associated with the aromatic ring and at 1020 cm^{-1} assigned to out-of-plane C–H bending of an alkene. These observations, taken together, suggest that C=C bonds form on alkyl chains during air-annealing (see below). The PL and PE spectral data for all the films, including these recast films, are summarized in Table 2.

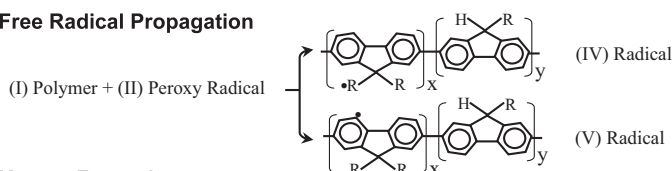
From these results, we conclude that increased fluorenone concentration is not, by itself, sufficient to account for the increased green-to-blue emission intensity ratio. Other factors must be significant and we propose that crosslinking accompanying thermal oxidation in air is important. The situation is somewhat similar to ladder-type poly(*para*-phenylene) (LPPP) that emits green light.^[10,22,23] Thermal degradation is a well-known issue in the polymer material aging process.^[24,25] The process typically involves thermally activated breaking of chemical bonds in the main and side chains. Recombining the fragments can lead to both smaller and larger molecular weight products. In the presence of oxygen, chain scission occurs more rapidly and reactions to form partially oxidized polymeric species, e.g., fluorenone, are possible.

In Scheme 2, we outline a likely chemical mechanism requiring oxygen to explain the enhanced green emission by thermal oxidation and crosslinking. While direct reaction of hydrocarbons with molecular oxygen is not favored, it is plausible that O_2 reacts with flaws in the polymer, especially when there is an H rather than an alkyl fragment attached to position 9 (Scheme 2). This reaction to remove H, likely catalyzed by residual transition metal catalysts, such as Ni, initiates a chain reaction by forming radicals (II) that react

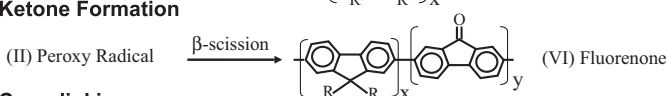
1. Initiation Step



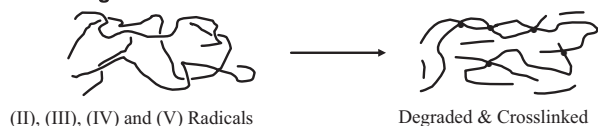
2. Free Radical Propagation



3. Ketone Formation



4. Crosslinking



Scheme 2. Proposed mechanisms for PFO degradation and crosslinking.

with oxygen to form peroxy radicals (III). The latter undergoes β -scission to form a carbonyl (VI) and abstract hydrogen to perpetuate the radical chain (IV) or (V). The formation of (IV) can lead to β -hydrogen elimination to form C=C as observed in the FTIR spectra. The observed crosslinking occurs as a result of chain termination by radical-radical combination.

3. Conclusions

In conclusion, the evidence suggests that the green emission of PFO-based conjugated polymers is correlated with the thermal oxidation degradation and crosslinking of PFO and is enhanced by annealing at elevated temperatures. The green emission originates from energy traps associated with one or more of the following: carbonyl groups (fluorenones) and bonds at crosslinking points. For thin (90 nm) films, the green-to-blue intensity ratio ($I_{\text{Green}}/I_{\text{Blue}}$) is 3.70, 4.35, and 1.54 for an air-annealed film, its insoluble residue (crosslinked), and a film cast from its soluble part (toluene is solvent), respectively. For thick (5–6 μm) film, the ratios are 13.33, 13.33, and 0.79, respectively. For these thick films FTIR analysis gives values of 0.018, 0.015, and 0.032, respectively, for the ratio of the concentration of carbonyl groups to aromatic rings. The film formed from the soluble portion exhibits a relatively low green emission but a high carbonyl concentration. This suggests that crosslinking plays an important role in driving up the green emission. The crosslinking apparently enhances excitation energy migration and energy transfer to the energy traps by hindering chain segment twisting and, consequently, improving the conjugativity and energy migration and energy transfer along the polymer network. Based on this model the observation that binary blends of PFO and high- T_g polymers suppress green emission^[16] is understood in terms of interrupting crosslinking even though oxidation may occur.

4. Experimental

The PFO-POSS (American Dye Sources) was used without further purification; the molecular structure is shown in Scheme 1. After dissolving in toluene to a concentration of 0.5 to 1.0 wt.-%, the solution was passed through a 0.45 μm poly(tetrafluoroethylene) (PTFE) filter. Two types of films were employed: 1. Thin films, 90 \pm 5 nm, were spin-cast. 2. Thick films, 5–6 μm , were prepared by dropping a controlled volume of solution from a micropipette onto substrates and allowing the solvent to evaporate. Substrates were 1 cm^2 pieces of microscope slides for PE and PL measurements and of Si wafers for XPS and FTIR. Before analysis, the films were dried at 60 $^\circ\text{C}$, below the glass-transition temperature of PFO-POSS, in a vacuum. Film thicknesses were measured by atomic force microscopy (AFM, CP Research Autoprobe, Thermomicroscopes, CA) and by profilometer (Alpha step 200, Tencor Instruments). Chemical characterization of the film (bulk and surface) relied on transmission infrared spectroscopy (Infinity Gold FTIR, Thermo-Mattson). The surface composition was determined using XPS (5700 ESCA, Physical Electronics).

Since control of the N_2 -annealing environment is, we believe, critical for understanding the emission characteristics, we describe our system and procedure in more detail. The vacuum oven with a base pressure of 2×10^{-3} torr was baked at 200 $^\circ\text{C}$ for 24 h and then cooled down to room temperature. Using a high flow rate of 99.99 % pure N_2 gas, to minimize exposure of the oven surfaces to O_2 , the oven door was opened, films were brought in swiftly (\sim 5 s), and the oven door closed. After evacuation to 2×10^{-3} torr, the temperature was increased over 2 h to 160 $^\circ\text{C}$. At this point, flowing N_2 at 1 atm was introduced and the temperature was raised to 200 $^\circ\text{C}$ and held for 2 h. After this anneal, the temperature was reduced to room temperature (several hours) while N_2 flow continued. Then the samples were removed for analysis.

The PE and PL spectra were recorded at front face (FF) geometry as the ratio of the sample signal to the reference signal on a SPEX DM3000 Fluorolog- τ 2 spectrofluorometer equipped with a 450 W xenon light source, Czerny-Turner double-grating excitation and emission monochromators and Hamamatsu R928 sample signal and reference photomultipliers. The width of excitation and emission monochromator slits was 1 mm (equivalent to 1.7 nm band width). In order to minimize photoreaction, Vincent Vszssto shuttles were inserted between excitation beam outlet and sample chamber, controlled by model 1976 accessory controller and DM3000F software through a UniBlitz D12.2 shutter drive. Subsequent analysis was performed using SPEX DM3000F software.

Gel permeation chromatography (GPC) data were collected using a system employing four μ -Styragel columns (pore size ranging from 500 to 10^5 \AA) connected in series and equipped with a Waters R401 differential refractometer, a Perkin Elmer LS fluorescence detector, and an HP 1050 UV-vis diode array connected in series. The GPC data was used to assess purity, molecular weight, and the molecular weight distribution. Degassed high-performance liquid chromatography (HPLC) grade THF was used as the mobile phase and polystyrene standards ($M_w/M_n < 1.06$, Pressure Chemical Company) were used for molecular weight and molecular weight distribution analysis.

Received: December 12, 2003
Final version: March 31, 2004

- [1] R. H. Friend, R. W. Gymer, A. B. Holmes, J. H. Burroughes, R. N. Marks, C. Taliani, D. D. C. Bradley, D. A. Dos Santos, J. L. Brédas, M. Lögdlund, W. R. Salaneck, *Nature* **1999**, 397, 121.
- [2] A. J. Heeger, *Solid State Commun.* **1998**, 107, 673.
- [3] A. Kraft, A. C. Grimsdale, A. B. Holmes, *Angew. Chem. Int. Ed.* **1998**, 37, 402.
- [4] M. T. Bernius, M. Inbasekaran, J. O'Brien, W. Wu, *Adv. Mater.* **2000**, 12, 1737.

- [5] X. Gong, P. K. Iyer, D. Moses, G. C. Bazan, A. J. Heeger, S. S. Xiao, *Adv. Funct. Mater.* **2003**, *13*, 325.
- [6] L. Romaner, A. Pogantsch, P. S. de Freitas, U. Scherf, M. Gaal, E. Zojer, E. J. W. List, *Adv. Funct. Mater.* **2003**, *13*, 597.
- [7] V. N. Bliznyuk, S. Carter, J. C. Scott, G. Klärner, R. D. Miller, D. C. Miller, *Macromolecules* **1999**, *32*, 36.
- [8] K. H. Weinfurter, H. Fujikawa, S. Tokito, Y. Taga, *Appl. Phys. Lett.* **2000**, *76*, 2502.
- [9] U. Scherf, E. J. W. List, *Adv. Mater.* **2002**, *14*, 477.
- [10] U. Lemmer, S. Heun, R. F. Mahrt, U. Scherf, M. Hopmeier, U. Siegner, E. O. Goebel, K. Muellen, H. Baessler, *Chem. Phys. Lett.* **1995**, *240*, 373.
- [11] F. Uckert, R. H. Tak, K. Müllen, H. Bässler, *Adv. Mater.* **2000**, *12*, 905.
- [12] S. Pannozzo, J.-C. Vial, Y. Kervalla, O. Stéphan, *J. Appl. Phys.* **2002**, *92*, 3495; and private communication.
- [13] L. M. Herz, R. T. Philips, *Phys. Rev. B* **2000**, *61*, 13 691.
- [14] G. Zeng, W. L. Yu, S. J. Chua, W. Huang, *Macromolecules* **2002**, *35*, 6907.
- [15] E. J. W. List, R. Guentner, P. S. de Freitas, U. Scherf, *Adv. Mater.* **2002**, *14*, 374.
- [16] A. P. Kulkarni, S. A. Jenekhe, *Macromolecules* **2003**, *36*, 5285.
- [17] S. Xiao, M. Nguyen, X. Gong, Y. Cao, H. Wu, D. Moses, A. J. Heeger, *Adv. Funct. Mater.* **2003**, *13*, 25.
- [18] M. Grell, D. D. C. Bradley, M. Inbasekaran, E. P. Woo, *Adv. Mater.* **1997**, *9*, 798.
- [19] L. S. Liao, M. K. Fung, C. S. Lee, S. T. Lee, M. Inbasekaran, E. P. Woo, W. W. Wu, *Appl. Phys. Lett.* **2000**, *76*, 3582.
- [20] R. T. Conley, *Infrared Spectroscopy*, Allyn and Bacon, Boston, MA **1966**.
- [21] M. R. Craig, M. M. de Kok, J. W. Hofstraat, A. P. H. J. Schenning, E. W. Meijer, *J. Mater. Chem.* **2003**, *13*, 2861.
- [22] J. M. Lupton, A. Pogantsch, T. Piok, E. J. W. List, S. Patil, U. Scherf, *Phys. Rev. Lett.* **2002**, *89*, 167 401.
- [23] M. Gaal, E. J. W. List, U. Scherf, *Macromolecules* **2003**, *36*, 4236.
- [24] G. W. Ehrenstein, *Polymeric Materials*, Hanser/Gardner, Cincinnati, OH **2001**.
- [25] H. Zweifel, *Stabilization of Polymeric Materials*, Springer, Berlin **1998**.